NISSUNA UMANA INVESTIGAZIONE SI PUO DIMANDARE VERA SCIENZIA
S'ESSA NON PASSA PER LE MATEMATICHE DIMOSTRAZIONI
LEONARDO DA VINCI

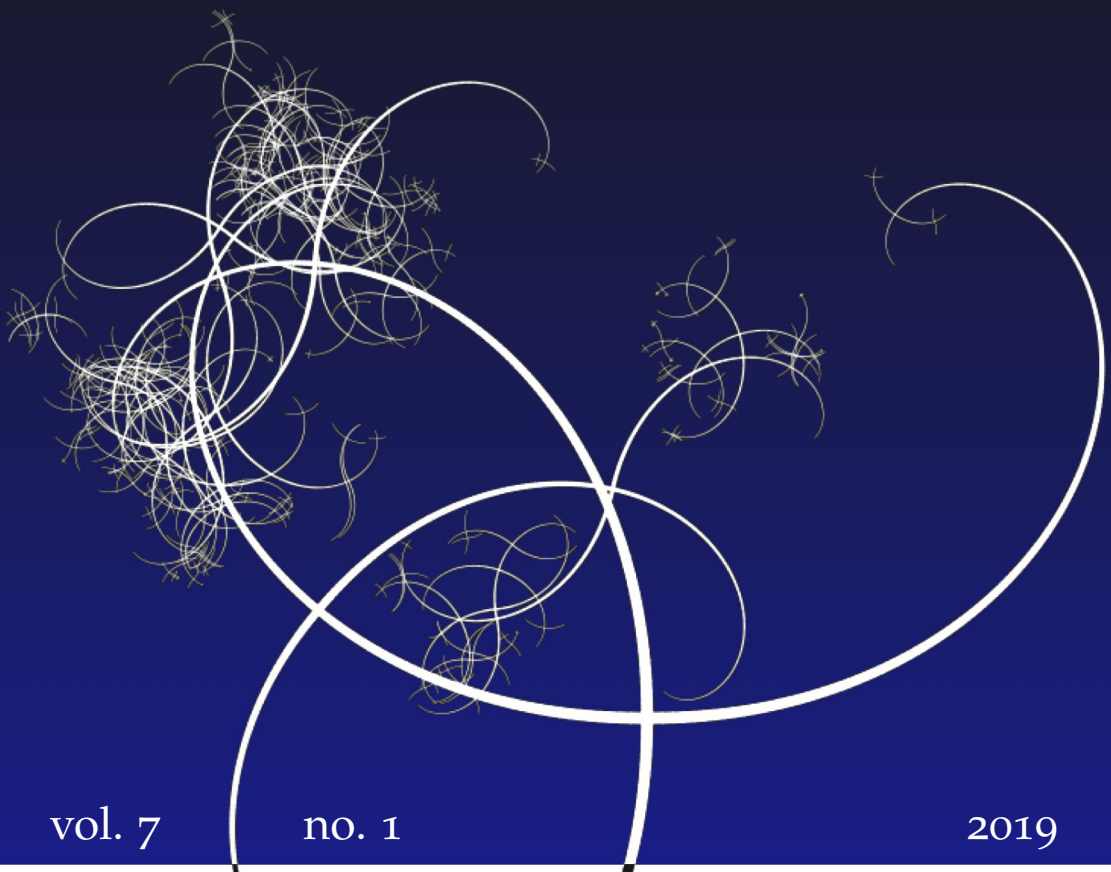

vol. 7 no. 1 2019

Mathematics and Mechanics *of* Complex Systems

Florence Browning and Harm Askes

ANALYTICAL SOLUTIONS FOR THE NATURAL FREQUENCIES OF RECTANGULAR SYMMETRIC ANGLE-PLY LAMINATED PLATES

msp

MATHEMATICS AND MECHANICS OF COMPLEX SYSTEMS
Vol. 7, No. 1, 2019
dx.doi.org/10.2140/memocs.2019.7.51

ANALYTICAL SOLUTIONS FOR THE NATURAL FREQUENCIES OF RECTANGULAR SYMMETRIC ANGLE-PLY LAMINATED PLATES

FLORENCE BROWNING AND HARM ASKES

Analytical solutions, based on the Ritz method, are derived for the lowest natural frequency of rectangular symmetric angle-ply laminated plates. Since symmetric angle-ply plates have nonzero cross-elasticity constants, the solutions are approximate. The accuracy of these solutions is tested with a convergence study using the Rayleigh quotient iteration method. With the solutions available in symbolic form, parameter studies are presented that establish the effect of plate aspect ratio and ply orientation angle for a number of stacking geometries. The results are also verified through a comparison with numerical Ritz solutions, showing a maximum error of 5% in our approximate solution.

1. Introduction

The focus of this paper is on the natural frequencies of rectangular anisotropic plates. Such plates often consist of layers the principal directions of which are aligned with the edges of the plates, but this restriction is not necessary — indeed, here we will focus on alternative arrangements. The stacking geometry affects the elastic properties of laminated plates, of which the lowest natural frequency is of particular relevance for serviceability criteria [Gsell et al. 2007].

To make qualitative and quantitative predictions of the mechanical behaviour of laminated plates, appropriate plate theory needs to be formulated. Starting from Kirchhoff–Love or Reissner–Mindlin theory, the heterogeneous effects of multiple layers of anisotropic material can be homogenised to arrive at an equivalent anisotropic plate theory; see for instance [Yang et al. 1966; Whitney and Leissa 1969; Leissa and Whitney 1970; Whitney 1972; Pagano 1969; 1970; Kulkarni and Pagano 1972]. These anisotropic plate models were discussed and compared to other modelling strategies for plates (and shells) by Noor et al. [1996]. Further refinements have also been developed; see for instance the 1980s work [Reddy 1984;

Communicated by Francesco dell'Isola.
PACS2010: 43.40.+s, 46.40.-f.
MSC2010: 74G10, 74H45.
Keywords: laminated plate, natural frequencies, anisotropy, elasticity.

Murakami 1986; Ren 1986] and the comparative studies [Carrera 2000; Stürzenbecher et al. 2010] of more recent years. The natural frequencies of laminated plates have been studied by Ohta and Ikuno [2002], who restricted their study to so-called cross-laminated plates (whereby the principal directions of each ply are parallel to the plate edges), and by Chaudhuri [2002] and Huang et al. [2006], who developed series-based analytical solutions that can be used for arbitrary layer geometries.

An aspect that has received relatively little attention in the literature (but for exceptions see [Hohe 2013]) is the effect of layer orientation on the natural frequencies of laminated plates, and in that context this paper will focus on so-called angle-ply plates, whereby every layer with a particular fibre orientation has a counterpart layer with the opposite fibre orientation. First, the relevant equations will be summarised briefly. The case of symmetric angle-ply plates is of interest, as the coupling of normal stresses to shear strains and vice versa leads to additional complexity that has, as far as the authors are aware, prohibited the establishment of a closed-form exact solution to date. Additional assumptions are required to formulate a simple approximate analytical solution; the validity of these assumptions is checked in a convergence study carried out in symbolic form with the Rayleigh quotient iteration method, which resulted in a novel set of Padé approximations. The results are also compared to numerical solutions obtained with the Ritz method, and a good agreement between the simple analytical solution and the two series solutions was observed. The usefulness and novelty of these solutions relies on their transparency — whilst the series-based solutions presented in [Chaudhuri 2002; Huang et al. 2006] can be expanded to arbitrary accuracy, they comprise lengthy expressions. For practical considerations and straightforward parameter studies a simpler solution with an upper limit to the error is often preferred.

2. Anisotropic plate theory

The anisotropic plate theory used in this paper builds on the seminal works of Whitney, Pagano, and their coworkers from the late 1960s and early 1970s. Membrane action and distributed loads will be ignored. Rectangular plates of length A, width B, and thickness H will be considered using the global Cartesian coordinate system shown in Figure 1. We will also define the aspect ratio α as $\alpha = A/B$.

For every individual ply, a local 1-2 coordinate system can be introduced whereby the 1-axis is aligned with the fibres, rotated along an angle θ from the x-axis. The stress-strain relation in local coordinates reads

$$\begin{bmatrix} \sigma_1 \\ \sigma_2 \\ \tau_{12} \end{bmatrix} = \begin{bmatrix} Q_{11} & Q_{12} & 0 \\ Q_{12} & Q_{22} & 0 \\ 0 & 0 & Q_{66} \end{bmatrix} \begin{bmatrix} \varepsilon_1 \\ \varepsilon_2 \\ \gamma_{12} \end{bmatrix}. \tag{1}$$

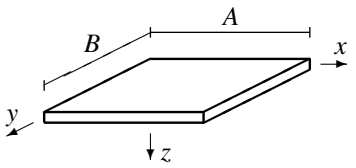

Figure 1. Global coordinate system and plate dimensions.

The constitutive coefficients Q_{ij} are written in terms of elastic constants as

$$Q_{11} = \frac{E_1}{1 - \nu_{12}\nu_{21}}, \tag{2a}$$

$$Q_{12} = \frac{\nu_{12}E_2}{1 - \nu_{12}\nu_{21}} = \frac{\nu_{21}E_1}{1 - \nu_{12}\nu_{21}}, \tag{2b}$$

$$Q_{22} = \frac{E_2}{1 - \nu_{12}\nu_{21}}, \tag{2c}$$

$$Q_{66} = G_{12}, \tag{2d}$$

where E_1 and E_2 are the Young's moduli parallel and perpendicular to the fibre direction, G_{12} is the shear modulus, and ν_{12} and ν_{21} are the Poisson's ratios associated with a stretch in the 1-direction and 2-direction, respectively.

The local stress-strain relations are translated to the global coordinate system, leading to

$$\begin{bmatrix} \sigma_{xx} \\ \sigma_{yy} \\ \tau_{xy} \end{bmatrix} = \begin{bmatrix} \overline{Q}_{11} & \overline{Q}_{12} & \overline{Q}_{16} \\ \overline{Q}_{12} & \overline{Q}_{22} & \overline{Q}_{26} \\ \overline{Q}_{16} & \overline{Q}_{26} & \overline{Q}_{66} \end{bmatrix} \begin{bmatrix} \varepsilon_{xx} \\ \varepsilon_{yy} \\ \gamma_{xy} \end{bmatrix}, \tag{3}$$

where

$$\overline{Q}_{11} = Q_{11}\cos^4\theta + (2Q_{12} + 4Q_{66})\cos^2\theta\sin^2\theta + Q_{22}\sin^4\theta, \tag{4a}$$

$$\overline{Q}_{22} = Q_{11}\sin^4\theta + (2Q_{12} + 4Q_{66})\cos^2\theta\sin^2\theta + Q_{22}\cos^4\theta, \tag{4b}$$

$$\overline{Q}_{12} = (Q_{11} + Q_{22} - 2Q_{12} - 4Q_{66})\cos^2\theta\sin^2\theta + Q_{12}, \tag{4c}$$

$$\overline{Q}_{66} = (Q_{11} + Q_{22} - 2Q_{12} - 4Q_{66})\cos^2\theta\sin^2\theta + Q_{66}, \tag{4d}$$

$$\overline{Q}_{16} = (Q_{11} - Q_{12} - 2Q_{66})\cos^3\theta\sin\theta + (Q_{12} - Q_{22} + 2Q_{66})\cos\theta\sin^3\theta, \tag{4e}$$

$$\overline{Q}_{26} = (Q_{11} - Q_{12} - 2Q_{66})\cos\theta\sin^3\theta + (Q_{12} - Q_{22} + 2Q_{66})\cos^3\theta\sin\theta. \tag{4f}$$

Note that the above transformation is expressed in terms of the engineering shear strain, not the tensorial shear strain, meaning that additional factors 2 and $\frac{1}{2}$ have been used compared to the usual transformation rules of second-order tensors.

The constitutive coefficients (4) are assumed to be piecewise constant for each ply. The heterogeneous response in the z-direction is homogenised by integrating

the stresses over the thickness of the plate, leading to the equation of transverse motion

$$D_{11}\frac{\partial^4 w}{\partial x^4} + (2D_{12} + 4D_{66})\frac{\partial^4 w}{\partial x^2 \partial y^2} + D_{22}\frac{\partial^4 w}{\partial y^4} + 4D_{16}\frac{\partial^4 w}{\partial x^3 \partial y} + 4D_{26}\frac{\partial^4 w}{\partial x \partial y^3} + \rho H \frac{\partial^2 w}{\partial t^2} = 0, \quad (5)$$

where w is the transverse displacement, ρ is the mass density, and H is the total thickness of the plate. Furthermore, the various plate bending coefficients D_{ij} are defined by

$$D_{ij} = \int_{-H/2}^{H/2} \bar{Q}_{ij} z^2 \, dz. \quad (6)$$

In case $D_{16} \neq 0$ and $D_{26} \neq 0$, an additional level of anisotropy is obtained in going from (1) to (3). These two coefficients are called the "cross-elasticity bending stiffness terms" [Whitney 1972]. In (5) this manifests itself in odd-order derivatives in terms of x and y, which has some implications for subsequent derivations, as will be explained below.

The boundary conditions for simply supported rectangular plates read

$$w = 0, \quad M_y = -D_{11}\frac{\partial^2 w}{\partial x^2} - 2D_{16}\frac{\partial^2 w}{\partial x \partial y} - D_{12}\frac{\partial^2 w}{\partial y^2} = 0 \quad \text{at } x = 0, A, \quad (7a)$$

$$w = 0, \quad M_x = -D_{12}\frac{\partial^2 w}{\partial x^2} - 2D_{26}\frac{\partial^2 w}{\partial x \partial y} - D_{22}\frac{\partial^2 w}{\partial y^2} = 0 \quad \text{at } y = 0, B, \quad (7b)$$

where M_x and M_y are the distributed moments (per unit of length) about the x-axis and y-axis, respectively.

3. Plate bending coefficients of symmetric angle-ply plates

In so-called angle-ply plates, each layer with orientation angle θ has a counterpart layer with orientation angle $-\theta$. Typical stacking sequences are symmetric or antisymmetric around the midplane $z = 0$. We will assume symmetric angle-ply plates with multiples of four layers in total, the same thickness for each layer, and alternating orientations of $+\theta$ and $-\theta$ for consecutive layers in each of the top half and bottom half of the plate. The standard plate bending coefficients can then be written as

$$D_{11} = \frac{H^3}{12}(Q_{11}\cos^4\theta + (2Q_{12} + 4Q_{66})\cos^2\theta \sin^2\theta + Q_{22}\sin^4\theta), \quad (8a)$$

$$D_{22} = \frac{H^3}{12}(Q_{11}\sin^4\theta + (2Q_{12} + 4Q_{66})\cos^2\theta \sin^2\theta + Q_{22}\cos^4\theta), \quad (8b)$$

$$D_{12} = \frac{H^3}{12}((Q_{11} + Q_{22} - 2Q_{12} - 4Q_{66}) \cos^2\theta \sin^2\theta + Q_{12}), \tag{8c}$$

$$D_{66} = \frac{H^3}{12}((Q_{11} + Q_{22} - 2Q_{12} - 4Q_{66}) \cos^2\theta \sin^2\theta + Q_{66}) \tag{8d}$$

irrespective of the actual number of layers, while the cross-elasticity plate bending coefficients read

$$D_{16} = \frac{H^3 \sin 2\theta}{8 \cdot n_{\text{layer}}}((Q_{11} - 2Q_{12} + Q_{22} - 4Q_{66}) \cos^2\theta - Q_{22} + Q_{12} + 2Q_{66}), \tag{8e}$$

$$D_{26} = -\frac{H^3 \sin 2\theta}{8 \cdot n_{\text{layer}}}((Q_{11} - 2Q_{12} + Q_{22} - 4Q_{66}) \cos^2\theta - Q_{11} + Q_{12} + 2Q_{66}) \tag{8f}$$

where n_{layer} is the total number of layers. It can be seen that the cross-elasticity coefficients vanish when the fibre orientations coincide with the Cartesian axes. Furthermore, the magnitude of the cross-elasticity coefficients reduces with an increased number of layers. Thus, the maximum effect of cross-elasticity is obtained for four layers, which will be assumed in the remainder of the paper.

4. Symmetric square angle-ply plate — a convergence study

In the presence of cross-elasticity, i.e., $D_{16} \neq 0$ and $D_{26} \neq 0$, it has been mentioned that an exact solution is not available [Jones 1999, p. 318]. Analytical solutions have been developed in [Chaudhuri 2002] and [Huang et al. 2006], but they are expressed in an extended series format, and a symbolic representation does not seem to be sufficiently transparent to be practicable. Instead, we have opted to use the Ritz method in symbolic form to generate an approximate solution to the cross-elasticity case.

The general solution for the Ritz method in the case of simply supported plates reads

$$w(x, y, t) = \sin(\omega t) \sum_{m=1}^{M} \sum_{n=1}^{N} C_{m,n} \sin\frac{m\pi x}{A} \sin\frac{n\pi y}{B}. \tag{9}$$

Adopting a square geometry, i.e., $A = B$, and using the same number of terms in both the x and y direction, i.e., $M = N$, the exact solutions of the Ritz problem for the lowest two values of M and N are denoted by $\omega^2_{(M,N)}$ and read

$$\omega^2_{(1,1)} = \frac{\pi^4 H^2 Q_{aa}}{12\rho B^4}, \tag{10a}$$

$$\omega^2_{(2,2)} = \frac{\pi^4 H^2 Q_{aa}}{12\rho B^4} \cdot \left(\frac{17}{2} - \frac{15}{2}\sqrt{1 + \frac{1024}{81}\frac{Q^2_{bb}}{Q^2_{aa}}}\right) \tag{10b}$$

where

$$Q_{aa} = Q_{11} + 2Q_{12} + Q_{22} + 4Q_{66} + (Q_{11} - 2Q_{12} + Q_{22} - 4Q_{66}) \sin^2 2\theta, \quad (11a)$$

$$Q_{bb} = (Q_{11} - Q_{22}) \frac{\sin 2\theta}{\pi^2} \quad (11b)$$

have been defined for a more compact notation.

For larger values of M and N, the size of the stiffness matrix becomes prohibitive to finding an exact solution in transparent symbolic form; thus, we have made two further approximations. Firstly, we have discarded any terms whereby $m \neq n$ — this can be justified by inspecting the eigenvector associated with (10b). Secondly, we have applied two iterations of the Rayleigh quotient iteration method to arrive at a relatively simple closed-form approximation of the lowest natural frequency.

(1) With trial eigenvector $\underline{v}_1 = [1, 0, 0, \ldots]^T$ we have computed the Rayleigh quotient RQ according to

$$\mathrm{RQ} = \frac{\underline{v}^T \boldsymbol{K} \underline{v}}{\underline{v}^T \boldsymbol{M} \underline{v}} \quad (12)$$

where $\boldsymbol{K}$ and $\boldsymbol{M}$ are the stiffness matrix and mass matrix, respectively. Not surprisingly, the value of the Rayleigh quotient in this first iteration equals the expression for ω^2 given in (10a).

(2) These values for $\underline{v}$ and RQ are used to compute an update on $\underline{v}$ according to

$$\underline{v}_2 = [\boldsymbol{K} - \mathrm{RQ} \cdot \boldsymbol{M}]^{-1} \underline{v}_1 \quad (13)$$

after which this new estimate of the eigenvector is used to recompute the Rayleigh quotient, and the resulting value of RQ is taken as an approximation for ω^2. Carrying out further iterations in symbolic form is possible in principle, but leads to expressions that are too unwieldy to be of practical use.

The above procedure has been executed for $M = N = 2$ up to $M = N = 5$, which gives the results in Table 1 on the next page. The first of these expressions, (15a), has been included to provide a comparison with the Ritz solution of (10b); the former is also a [1, 1]-Padé approximation of the latter, following $\sqrt{1+x} \approx (4+3x)/(4+x)$.

To estimate the differences between the various solutions, it is first established that the ratio Q_{bb}/Q_{aa} adopts its maximum value for $\theta = \frac{1}{4}\pi$; in particular

$$\frac{Q_{bb}}{Q_{aa}} = \frac{1}{2\pi^2} \cdot \frac{E_1 - E_2}{E_1 + E_2} \quad \text{at } \theta = \tfrac{1}{4}\pi, \quad (14)$$

which in turn adopts its maximum value for vanishing E_2. With the estimate $Q_{bb}/Q_{aa} < 1/2\pi^2$, the relative difference between (15a) and (10b) is less than

$$\omega^2_{(2,2)} \approx \frac{\pi^4 H^2 Q_{aa}}{12\rho B^4} \cdot \frac{81 - 3584\, Q^2_{bb}/Q^2_{aa}}{81 + 256\, Q^2_{bb}/Q^2_{aa}}, \tag{15a}$$

$$\omega^2_{(3,3)} \approx \frac{\pi^4 H^2 Q_{aa}}{12\rho B^4} \cdot \frac{1 - 128\, Q^2_{bb}/Q^2_{aa} + 3787\, Q^4_{bb}/Q^4_{aa}}{1 - 81\, Q^2_{bb}/Q^2_{aa} + 1793\, Q^4_{bb}/Q^4_{aa}}, \tag{15b}$$

$$\omega^2_{(4,4)} \approx \frac{\pi^4 H^2 Q_{aa}}{12\rho B^4} \cdot \frac{1 - 205\, Q^2_{bb}/Q^2_{aa} + 11457\, Q^4_{bb}/Q^4_{aa} - 103802\, Q^6_{bb}/Q^6_{aa}}{1 - 157\, Q^2_{bb}/Q^2_{aa} + 6251\, Q^4_{bb}/Q^4_{aa} + 3625\, Q^6_{bb}/Q^6_{aa}}, \tag{15c}$$

$$\omega^2_{(5,5)} \approx \frac{\pi^4 H^2 Q_{aa}}{12\rho B^4} \cdot \frac{1 - 281\, Q^2_{bb}/Q^2_{aa} + 24601\, Q^4_{bb}/Q^4_{aa} - 681845\, Q^6_{bb}/Q^6_{aa} + 5045965\, Q^8_{bb}/Q^8_{aa}}{1 - 233\, Q^2_{bb}/Q^2_{aa} + 15876\, Q^4_{bb}/Q^4_{aa} - 266394\, Q^6_{bb}/Q^6_{aa} + 1438407\, Q^8_{bb}/Q^8_{aa}}. \tag{15d}$$

Table 1. Approximate natural frequencies for the Ritz problem in the cross-elasticity case: symmetric square, modes with $M = N$ ranging from 2 through 5.

10^{-5}, which indicates that the Rayleigh quotient iteration method provides an excellent approximation of the Ritz solution. Comparing (15b), (15c), and (15d) to (10b) leads to maximum relative errors of 1.5%, 2.4%, and 2.7%, respectively.

These results are obviously encouraging, but they must be interpreted with some caution. Whilst it is well-known that the Rayleigh quotient iteration method converges very rapidly (also confirmed by the comparison above for $M = N = 2$), it must be kept in mind that these results are obtained using two iterations only. Furthermore, the Ritz method itself is known to converge much slower than other methods such as direct Fourier series [Whitney 1972], although convergence is better for plates that are simply supported on all sides. Applying the Rayleigh quotient iteration method in symbolic form could be used to increase the accuracy of the analytical solution, but instead of seeking a solution in series format we will next use the Ritz method with $M = N = 2$ below to extend the analysis to rectangular plates.

5. Rectangular angle-ply plates

Using (9) with $M = N = 2$ leads to a stiffness matrix $\boldsymbol{K}$ and mass matrix $\boldsymbol{M}$ as

$$\boldsymbol{K} = \begin{bmatrix} K_{11} & 0 & 0 & K_{14} \\ 0 & K_{22} & K_{23} & 0 \\ 0 & K_{23} & K_{33} & 0 \\ K_{14} & 0 & 0 & K_{44} \end{bmatrix} \quad \text{and} \quad \boldsymbol{M} = \frac{\rho H B^2 \alpha}{4} \boldsymbol{I} \tag{16}$$

where $\boldsymbol{I}$ is the identity matrix. Noting that $K_{44} = 16K_{11}$, the lowest natural

	E_1 [GPa]	E_2 [GPa]	ν_{12}	ν_{21}	G_{12} [GPa]	ρ [kg/m^3]
GFR composite	46.2	16.6	0.26	0.093	6.9	2027
spruce	11.0	0.37	0.44	0.015	0.69	500

Table 2. Material properties for a glass-fibre reinforced composite and spruce.

frequency is found from

$$\omega = \sqrt{\frac{34K_{11} - 2\sqrt{225K_{11}^2 + 4K_{14}^2}}{\rho H B^2 \alpha}} \tag{17}$$

where the relevant stiffness matrix components are given in terms of the plate bending coefficients as

$$K_{11} = \frac{\pi^4}{4B^2\alpha^3}(D_{11} + (2D_{12} + 4D_{66})\alpha^2 + D_{22}\alpha^4), \tag{18a}$$

$$K_{14} = -\frac{160\pi^2}{9B^2\alpha^2}(D_{16} + D_{26}\alpha^2). \tag{18b}$$

For quantitative comparisons, we will use the two sets of material parameters listed in Table 2, associated respectively with a glass-fibre reinforced (GFR) composite [Fällström et al. 1996] and spruce [Stürzenbecher et al. 2010].

The natural frequencies according to (17) have been plotted in Figure 2 for a

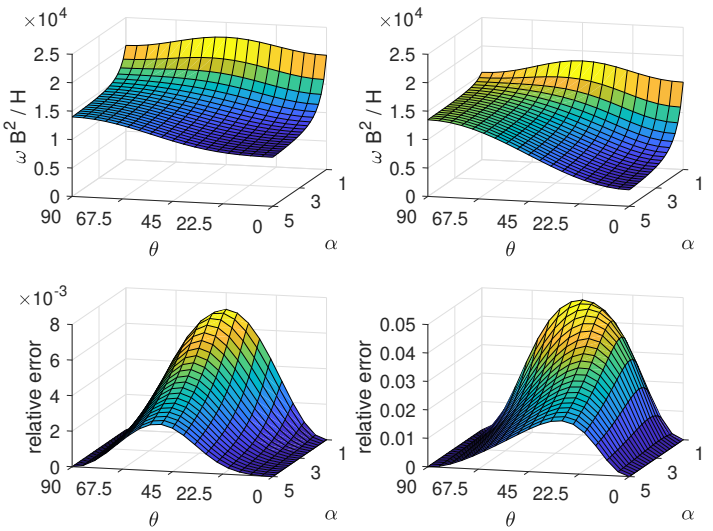

Figure 2. Normalised natural frequency ω (top) and relative error of the analytical solution (bottom) against plate aspect ratio α and fibre orientation angle θ. Left: GFR composite; right: spruce.

range of plate aspect ratios and fibre orientation angles, and for the two sets of material parameters given in Table 2 — note that the fibre orientation angle is plotted in degrees, not radians. The approximate solutions of (17) have also been compared to solutions obtained numerically with the Ritz method using $M = N = 50$.

The natural frequencies for the two sets of material data are qualitatively very similar. The maximum frequency is found for $\theta = \frac{1}{4}\pi$ in case of aspect ratios close to unity, and for $\theta = \frac{1}{2}\pi$ in case of larger aspect ratios. The dependence on the aspect ratio is strongest for $\theta = 0$, i.e., when the fibres are spanning the larger dimension — particularly for spruce, which has a larger E_1/E_2 ratio. The quantitative differences between the GFR composite and spruce are due to the much stronger degree of anisotropy encountered in spruce. This also impacts the accuracy of the approximate solution given in (17). The relative error of the analytical solution with respect to the benchmark numerical solution is seen to be less than 1% for the GFR composite, but more than five times as high for spruce. Nevertheless, a 5% error only occurs for aspect ratio $\alpha = 1$ and fibre orientations $\theta = \frac{1}{4}\pi$ (which is also the geometry for which maximum errors were studied in Section 4), whereas other combinations of α and θ lead to (much) lower errors. This level of accuracy is deemed to be proportionate and acceptable, given the simplicity and transparency of (17) and (18).

6. Conclusions

Simple and transparent expressions for the lowest natural frequency have been derived for rectangular anisotropic plates. Since the plate behaviour includes a coupling between normal stresses and shear strains (and vice versa), a phenomenon known as “cross-elasticity”, the solutions are approximate. A rudimentary convergence study in symbolic form based on the Rayleigh quotient iteration method has confirmed that a relatively low order of the Ritz method can be used for cases that are simply supported on all sides. This has been employed for more general plate configurations with cross-elasticity; because the solutions are obtained in symbolic form, parameter studies are straightforward. The accuracy of the method has been further confirmed by comparison with numerically obtained Ritz solutions.

Due to the chosen approach of seeking closed-form solutions, certain simplifications and assumptions had to be made. Thus, we have studied only one set of boundary conditions, namely simply supported on all sides, we have ignored membrane action, and cross-sectional warping has not been included. These effects, and others, can be studied using a numerical solution approach in combination with a more sophisticated plate theory, whereby the analytical solutions provided in this paper may serve as reference solutions.

Acknowledgements

We are indebted to Doctor Karin de Borst (Shell, The Netherlands) and Professor Ilanko (University of Waikato, New Zealand) for kindly providing insightful comments on an earlier draft.

References

[Carrera 2000] E. Carrera, "An assessment of mixed and classical theories on global and local response of multilayered orthotropic plates", *Compos. Struct.* **50**:2 (2000), 183–198.

[Chaudhuri 2002] R. A. Chaudhuri, "On the roles of complementary and admissible boundary constraints in Fourier solutions to the boundary value problems of completely coupled rth order PDEs", *J. Sound Vib.* **251**:2 (2002), 261–313.

[Fällström et al. 1996] K.-E. Fällström, K. Olofsson, H. O. Saldner, and S. Schedin, "Dynamic material parameters in an anisotropic plate estimated by phase-stepped holographic interferometry", *Opt. Laser. Eng.* **24**:5–6 (1996), 429–454.

[Gsell et al. 2007] D. Gsell, G. Feltrin, S. Schubert, R. Steiger, and M. Motavalli, "Cross-laminated timber plates: evaluation and verification of homogenized elastic properties", *J. Struct. Eng.* **133**:1 (2007), 132–138.

[Hohe 2013] J. Hohe, "Effect of core and face sheet anisotropy on the natural frequencies of sandwich shells with composite faces", *Int. J. Compos. Mater.* **3**:6B (2013), 40–52.

[Huang et al. 2006] Y. Huang, Y. J. Lei, and H. J. Shen, "Free vibration of anisotropic rectangular plates by general analytical method", *Appl. Math. Mech.* **27**:4 (2006), 461–467.

[Jones 1999] R. M. Jones, *Mechanics of composite materials*, 2nd ed., Taylor & Francis, New York, 1999.

[Kulkarni and Pagano 1972] S. V. Kulkarni and N. J. Pagano, "Dynamic characteristics of composite laminates", *J. Sound. Vib.* **23**:1 (1972), 127–143.

[Leissa and Whitney 1970] A. W. Leissa and J. M. Whitney, "Analysis of a simply supported laminated anisotropic rectangular plate", *AIAA J.* **8**:1 (1970), 28–33.

[Murakami 1986] H. Murakami, "Laminated composite plate theory with improved in-plane responses", *J. Appl. Mech.* **53**:3 (1986), 661–666.

[Noor et al. 1996] A. K. Noor, W. S. Burton, and C. W. Bert, "Computational models for sandwich panels and shells", *Appl. Mech. Rev.* **49**:3 (1996), 155–199.

[Ohta and Ikuno 2002] Y. Ohta and T. Ikuno, "The study of analytical models for vibration of cross-ply laminated thick plates", *JSME Int. J. C* **45**:1 (2002), 107–112.

[Pagano 1969] N. J. Pagano, "Exact solutions for composite laminates in cylindrical bending", *J. Compos. Mater.* **3**:3 (1969), 398–411.

[Pagano 1970] N. J. Pagano, "Exact solutions for rectangular bidirectional composites and sandwich plates", *J. Compos. Mater.* **4**:1 (1970), 20–34.

[Reddy 1984] J. N. Reddy, "A simple higher-order theory for laminated composite plates", *J. Appl. Mech.* **51**:4 (1984), 745–752.

[Ren 1986] J. G. Ren, "A new theory of laminated plate", *Compos. Sci. Tech.* **26**:3 (1986), 225–239.

[Stürzenbecher et al. 2010] R. Stürzenbecher, K. Hofstetter, and J. Eberhardsteiner, "Structural design of Cross Laminated Timber (CLT) by advanced plate theories", *Compos. Sci. Tech.* **70**:9 (2010), 1368–1379.

[Whitney 1972] J. M. Whitney, "On the analysis of anisotropic rectangular plates", technical report AD-776 017, Air Force Materials Laboratory, 1972, Available at http://www.dtic.mil/dtic/tr/fulltext/u2/776017.pdf.

[Whitney and Leissa 1969] J. M. Whitney and A. W. Leissa, "Analysis of heterogeneous anisotropic plates", *J. Appl. Mech.* **36**:2 (1969), 261–266.

[Yang et al. 1966] P. C. Yang, C. H. Norris, and Y. Stavsky, "Elastic wave propagation in heterogeneous plates", *Int. J. Solid. Struct.* **2**:4 (1966), 665–684.

Received 17 Jul 2018. Revised 29 Aug 2018. Accepted 24 Oct 2018.

FLORENCE BROWNING: florence.browning22@gmail.com
Interrobang Architecture and Engineering, Webb Yates Engineers Ltd, London, United Kingdom

HARM ASKES: h.askes@sheffield.ac.uk
Department of Civil and Structural Engineering, University of Sheffield, Sheffield, United Kingdom